Supplementary Information for

Calix[4]arenes in Mixed Protic Media: Conformational Characteristics and Solvent Effects Captured with Molecular Simulations

Rakiba Rohman,*[a] and Neelanjana Sengupta*[a]

[a.] Department of Biological Sciences, Indian Institute of Science Education and Research Kolkata, Mohanpur, West Bengal 741246, India

Email: n.sengupta@iiserkol.ac.in and raqiba.rohman444@gmail.com

Contents

Figures

Tables

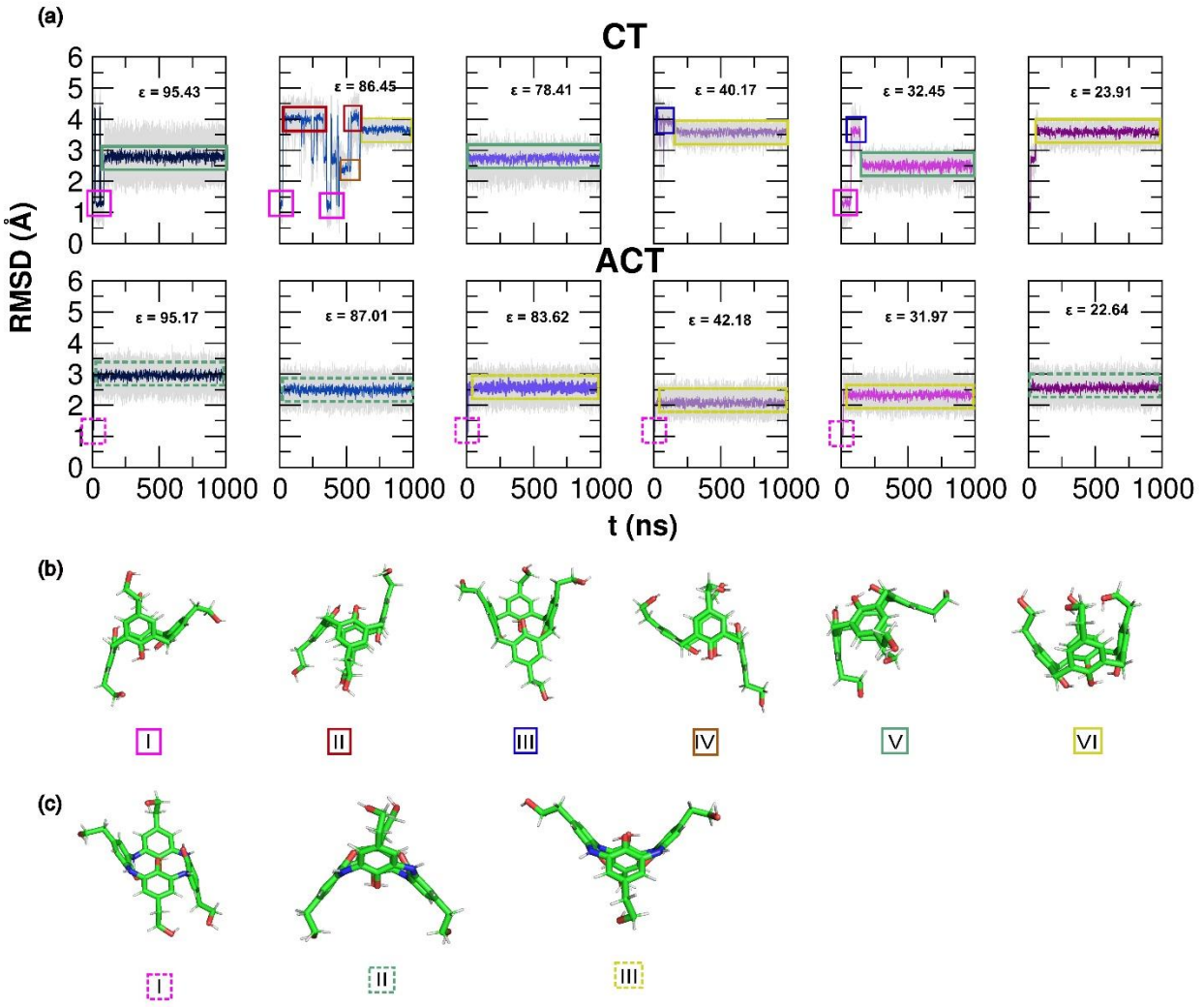

Fig. S1 (a) Root Mean Square Deviation (RMSD, in Å) of calixtyrosol (CT, upper panel) and aza-calixtyrosol (ACT, lower panel) as a function of simulation time (t), for a range of effective dielectric constants (ε_{eff}). Each subplot corresponds to a different dielectric condition, with grey traces representing instantaneous RMSD values and colored lines denoting running averages. (b) and (c) represent snapshots of the structures corresponding to the distinct distributions of the RMSD plots. The structures numbered with the *magenta* color code correspond to the starting structure at the beginning of the unconstrained production run, whereas those numbered with the *green* and *yellow* are obtained at the end of 1000ns of production run.

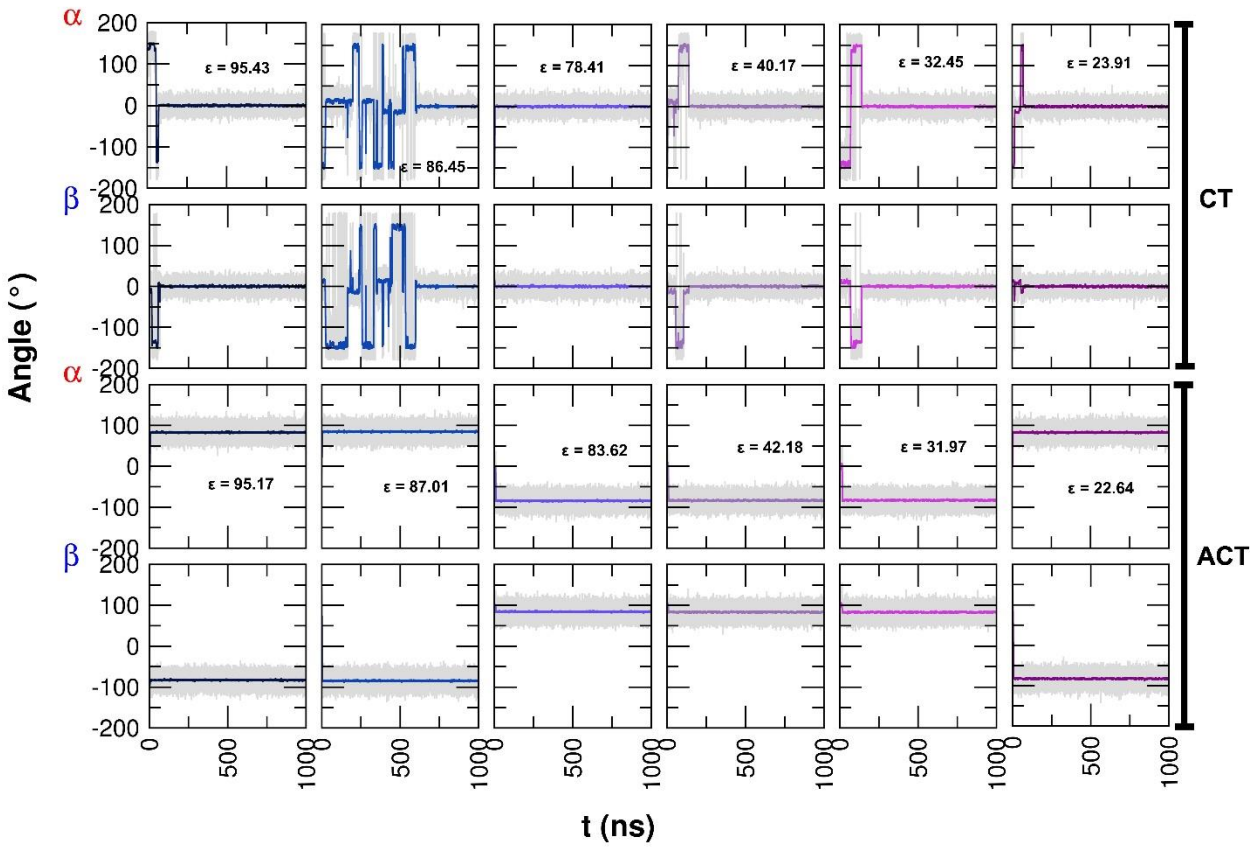

Fig. S2 Time evolution of key dihedral angles α and β in calix[4]tyrosol (CT, top two rows) and aza-calix[4]tyrosol (ACT, bottom two rows) across a range of ε_{eff}, representing different solvent environments. In each panel, grey lines show the raw angle values sampled throughout 1 microsecond molecular dynamics simulations, while the colored traces depict the corresponding running averages. The plots illustrate the dynamic behavior and stability of the characteristic conformational angles under various solvent polarities.

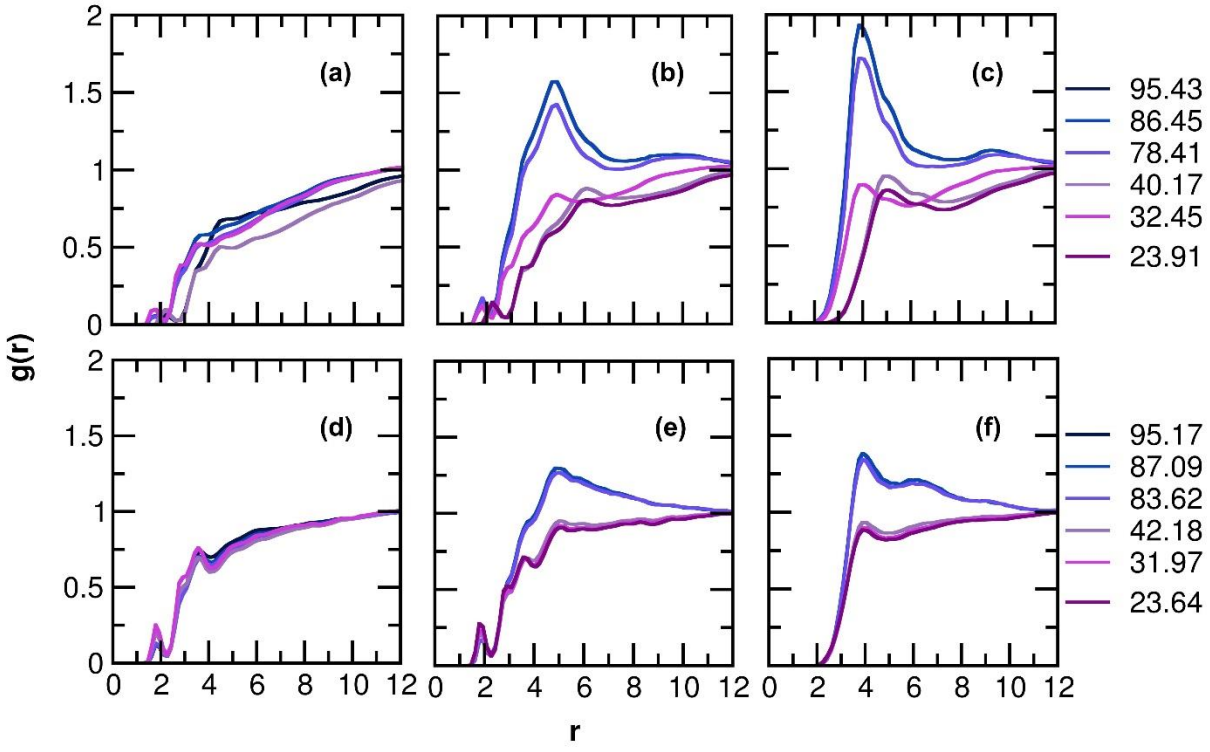

Fig. S3 Representation of radial distribution functions (RDFs), $g(r)$, (r is in Å) for the oxygen atoms of water [H_2O(O)], oxygen atoms of methanol [MeOH(O)], and carbon atoms of methanol [MeOH(C)], respectively, measured relative to all atoms of CT (upper row) and ACT (lower row) calixaromatics under various ε_{eff}.

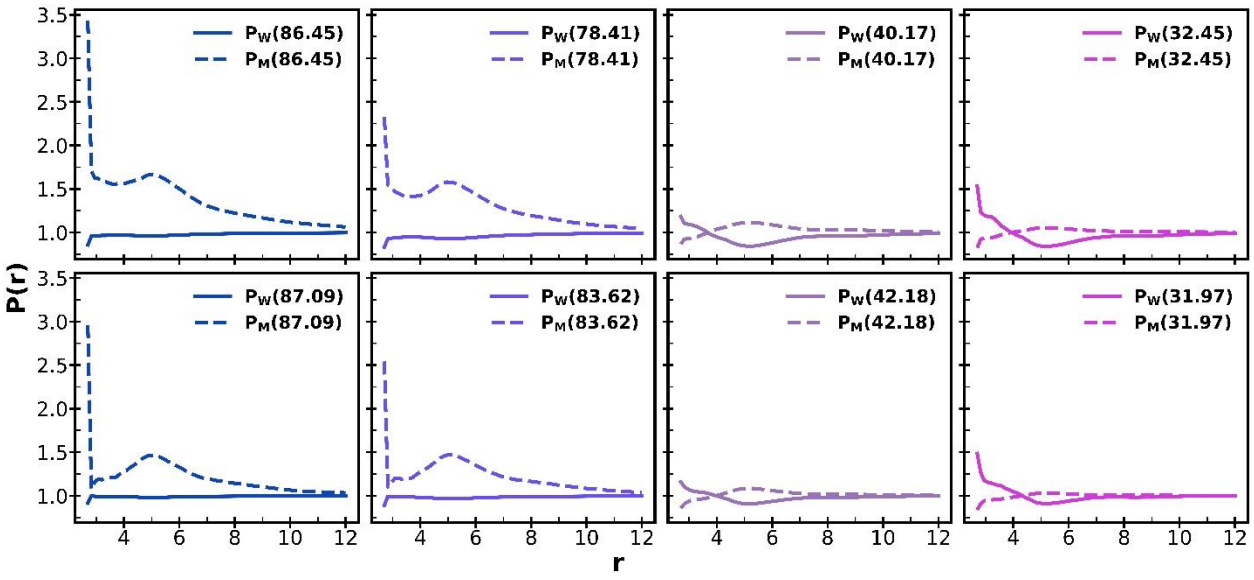

Fig. S4 Preferential interaction parameter, $P(r)$, (r is in Å) for water [P_W, solid line] and methanol [P_M, dashed line] oxygen atoms with respect to CT (top row) and ACT (bottom row) as a function of distance r from the macrocycle, calculated under varying ε_{eff}.

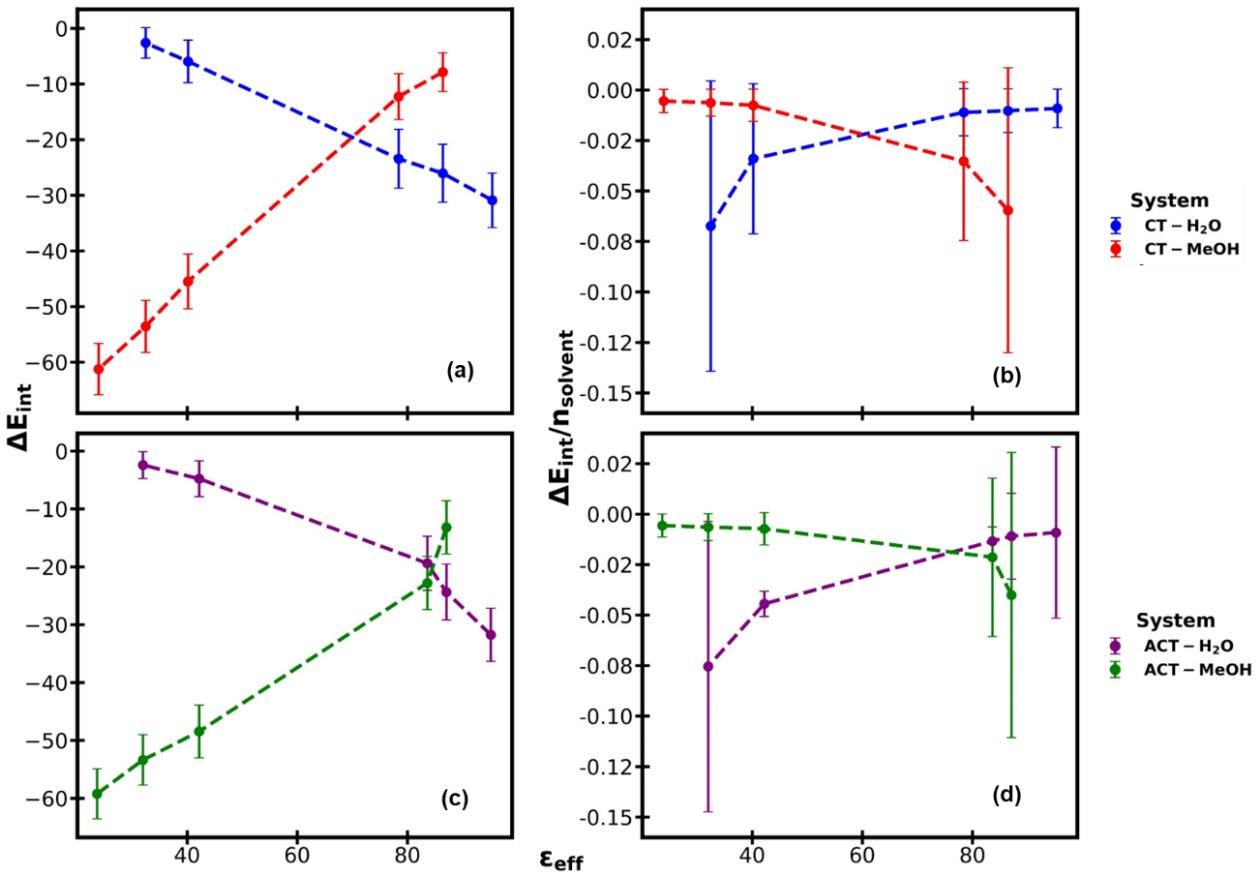

Fig. S5 Variation of interaction energies (ΔE_{int}, kcal/mol) and interaction energy per solvent molecule ($\Delta E_{\text{int}}/n_{\text{solvent}}$, kcal/mol) between CT or ACT and solvation shell solvent molecules as a function of ε_{eff}. [(a) and (c)] represent the total interaction energy of water and methanol in the solvation shells with CT (a) and ACT (c). [(b) and (d)] is the corresponding interaction energies normalized per solvent molecule.

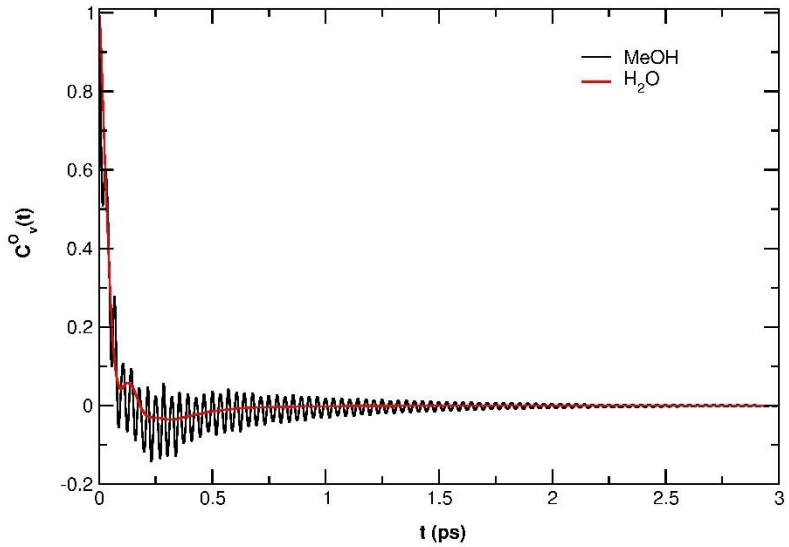

Fig. S6 The normalized velocity autocorrelation functions (VACF) of oxygen atoms, $C_v^O(t)_{\mathrm{H_2O}}$, of H_2O and MeOH as a function of time t (in ps)

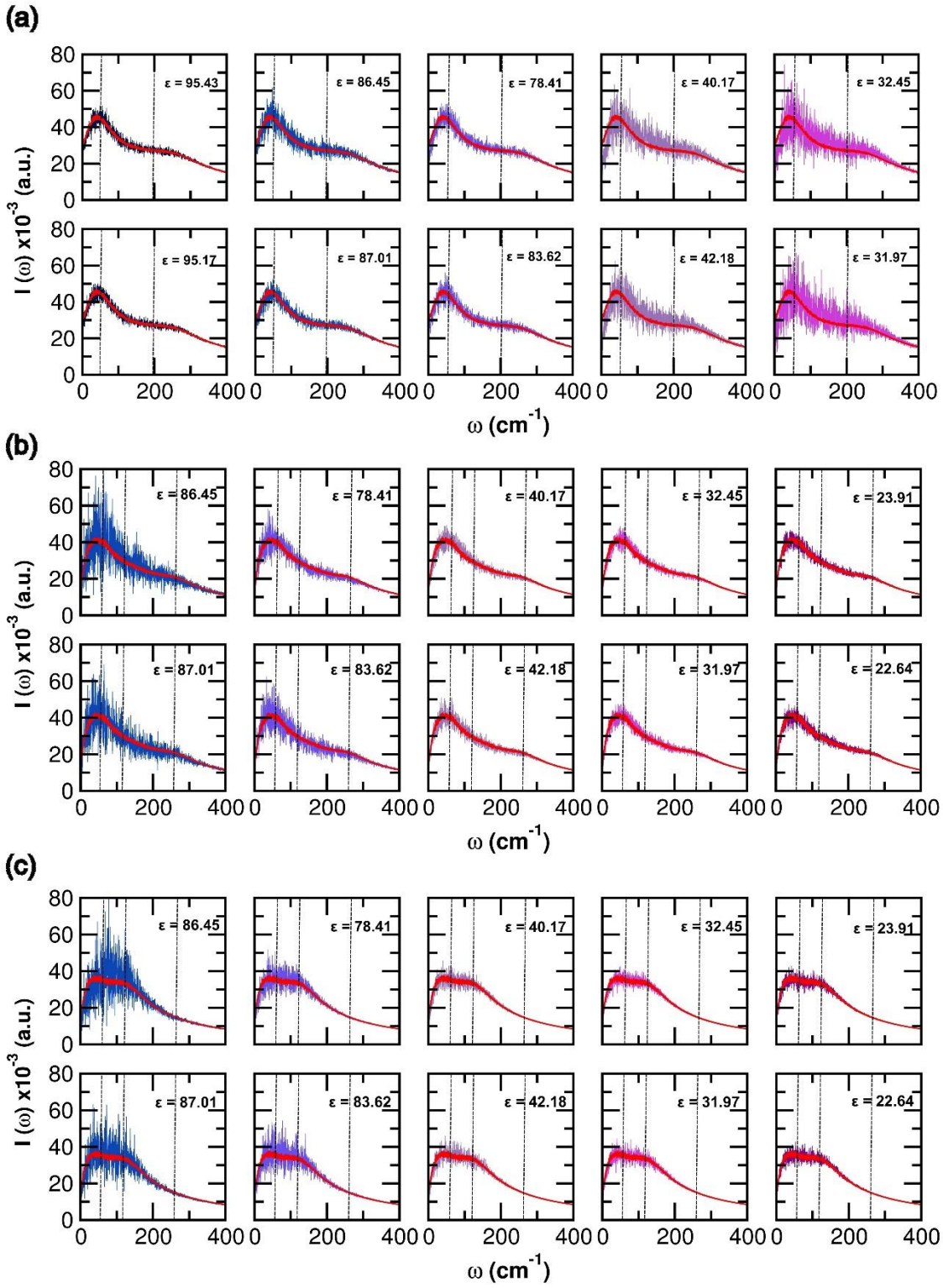

Fig. S7 Vibrational density of states (VDoS), $I(\omega)$ (a.u.), as a function of frequency ω (cm^{-1}), obtained from the Fourier transformation of the VACF. (a) represents VDoS plots of hydration

layer water (oxygen atom), (b) and (c) represent the same for solvation layer methanol (oxygen and carbon atoms, respectively). The red line represents the respective bulk systems.

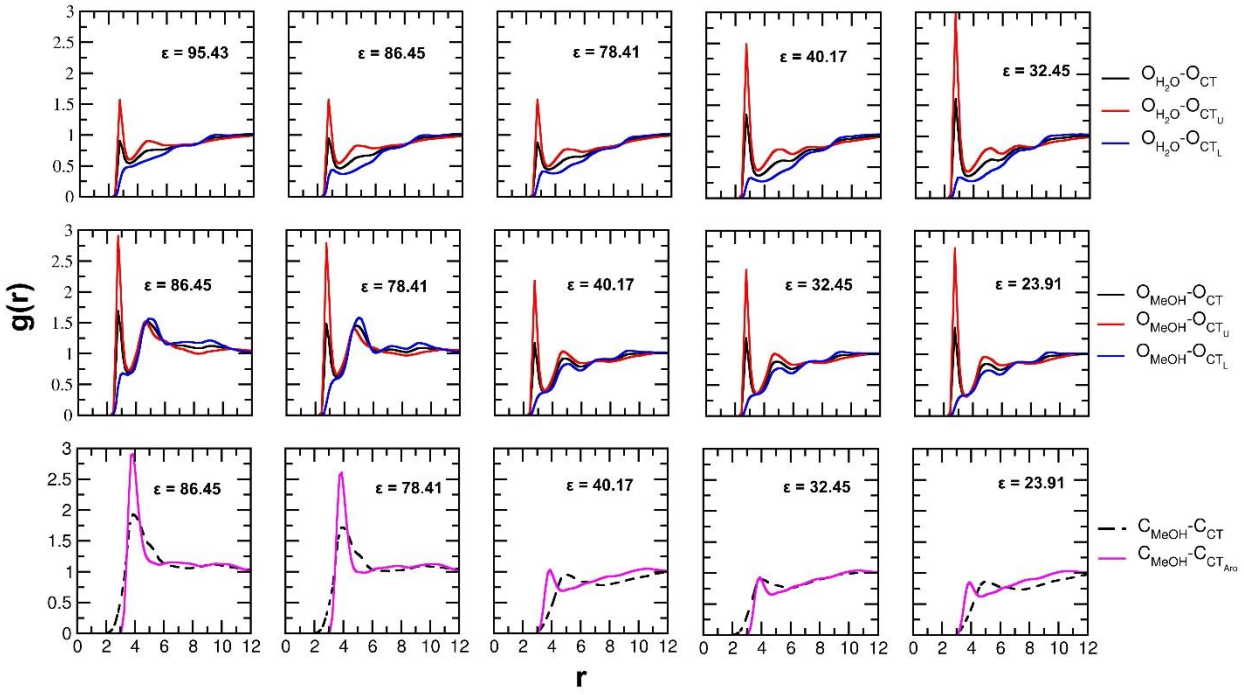

Fig. S8 Representation of RDFs (r is in Å) for heavy atoms of water and methanol relative to distinct structural regions of CT. For each ε_{eff}, water and methanol atoms (top row: O_{H2O}–CT, middle row: O_{MeOH}–CT, bottom row: C_{MeOH}–CT) are analyzed around three distinct parts of the calix[4]aromatic structure: whole calixaromatic (CT), upper rim (CT_U), lower rim (CT_L), and aromatic ring (CT_{Aro})

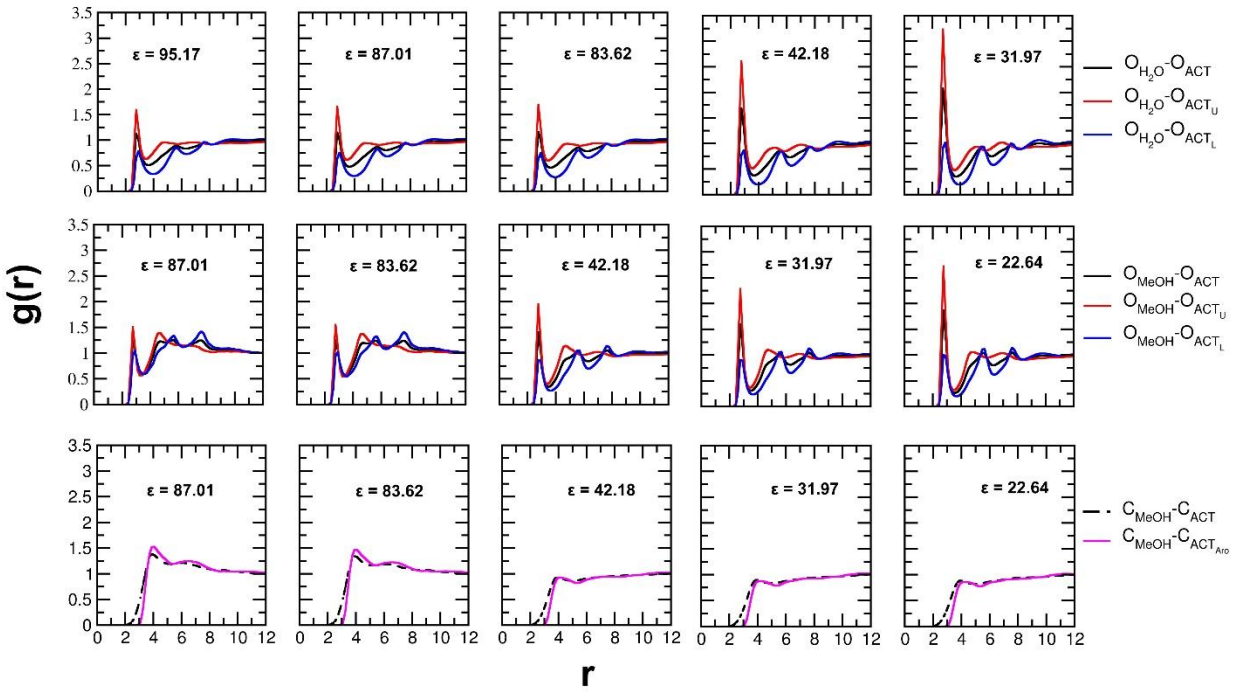

Fig. S9 Representation of RDFs (r is in Å) for heavy atoms of water and methanol relative to distinct structural regions of ACT. For each ε_{eff}, water and methanol atoms (top row: O_{H2O}–ACT, middle row: O_{MeOH}–ACT, bottom row: C_{MeOH}–ACT) are analyzed around three distinct parts of the calix[4]aromatic structure: whole calixaromatic (ACT), upper rim (ACT_U), lower rim (ACT_L), and aromatic ring (ACT_{Aro})

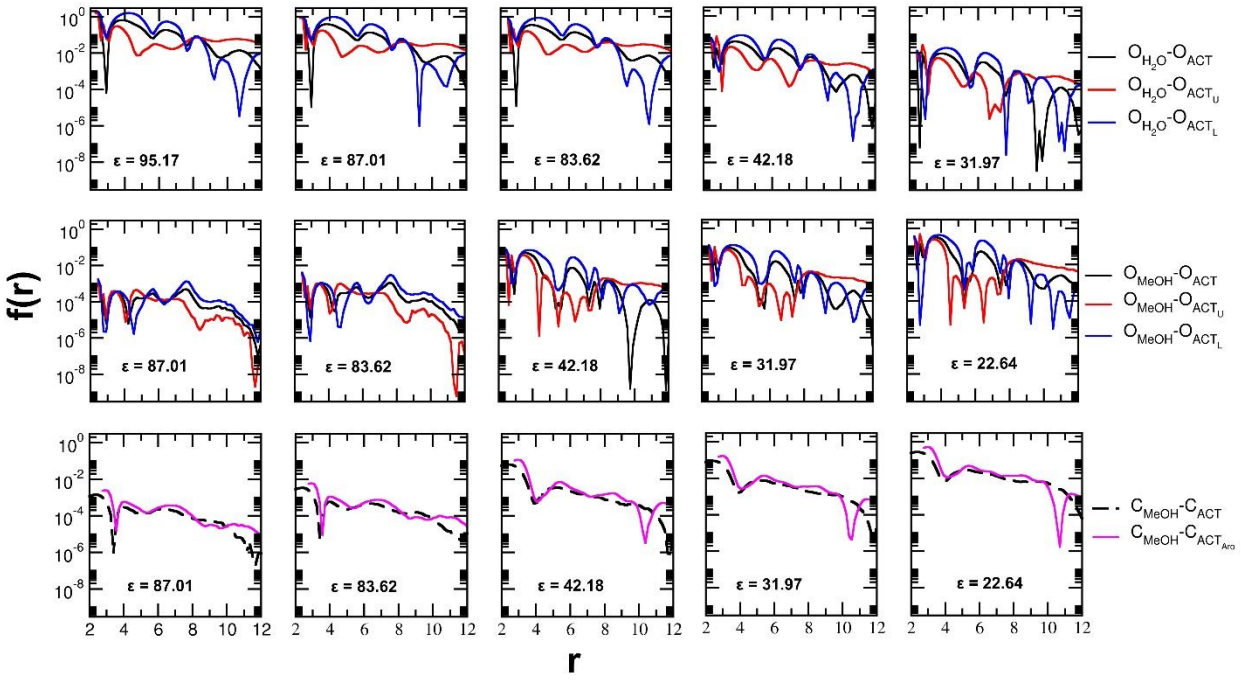

Fig. S10 Representation of site-resolved pair entropy parameter, $f(r)$, (r is in Å) for water and methanol atoms relative to distinct structural regions of ACT. For each ε_{eff}, water and methanol atoms (top row: O_{H2O}–ACT, middle row: O_{MeOH}–ACT, bottom row: C_{MeOH}–ACT) are analyzed around three distinct parts of the calix[4]aromatic structure: whole calixaromatic (ACT), upper rim (ACT_U), lower rim (ACT_L), and aromatic ring (ACT_{Aro})

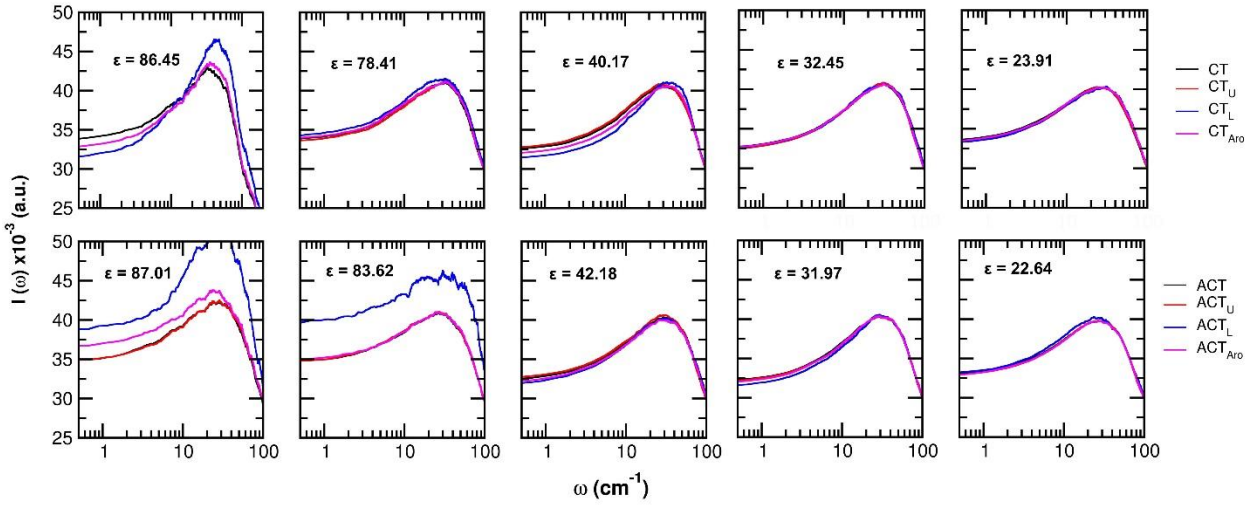

Fig. S11 Vibrational density of states (VDoS), $I(\omega)$ (a.u.), for solvation shell methanol oxygen atoms resolved by the local region around CT (top row) and ACT (bottom row). For each ε_{eff}, spectra are compared for methanol O atoms in proximity to the whole macrocycle, upper rim, lower rim, and aromatic ring regions. The x-axis is plotted on a logarithmic scale to emphasize low-frequency vibrational modes.

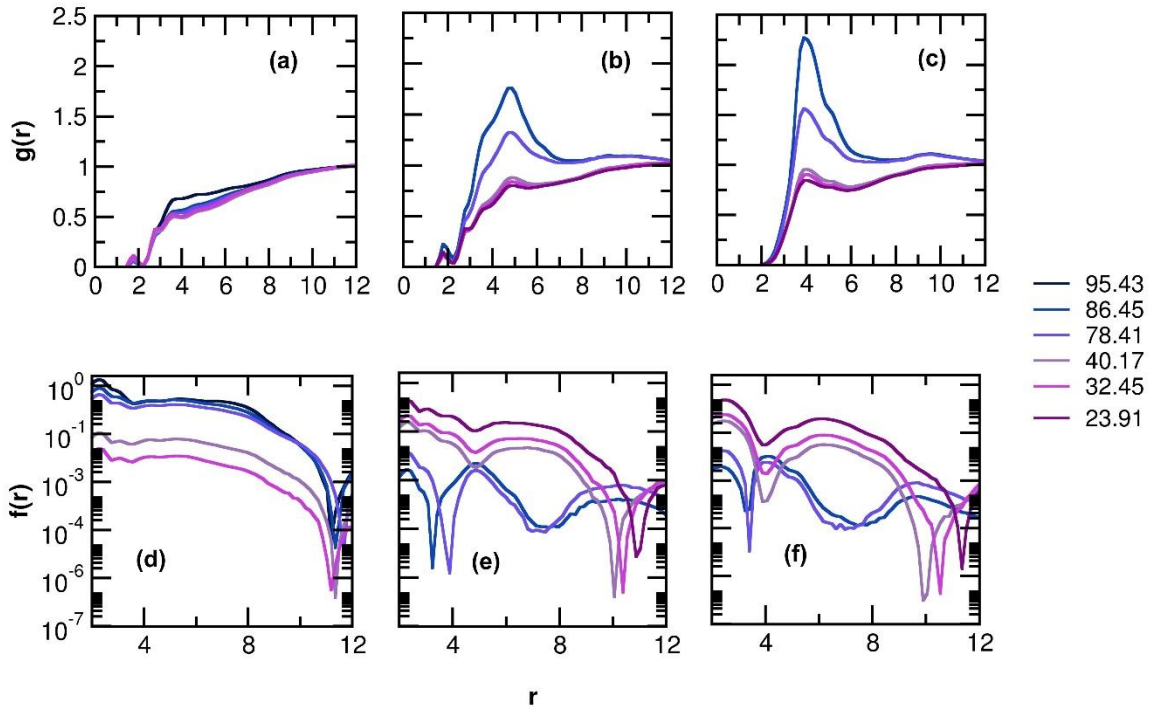

Fig. S12 Representation of radial distribution functions (RDFs), $g(r)$ [(a), (b), (c)], and time-averaged pair entropy parameter, $f(r)$ [(d), (e), (f)], (r is in Å) for the oxygen atoms of water [H_2O(O)], oxygen atoms of methanol [MeOH(O)], and carbon atoms of methanol [MeOH(C)], respectively, measured relative to all atoms of CT under various ε_{eff}, obtained from repeated simulation trajectory.

Table S1 The percentage composition of methanol and the effective dielectric constant of the solvent media (ε_{eff}) in various solvent mixtures

MeOH (%n/n)	ε_{eff}	
	CT	ACT
0	95.43	95.17
5	86.45	87.09
10	78.41	83.62
55	40.17	42.18
75	32.45	31.97
100	23.91	23.64

Table S2 Mean peak positions (in cm^{-1}) of the VDoS bands for water

CT		
ε_{eff}	ω_1	ω_2
95.43	54.23	200.02
86.45	54.22	200.14
78.41	55.12	200.60
40.17	55.17	199.61
32.45	54.79	198.72
23.91	---	---
ACT		
95.17	55.88	199.06
87.09	54.55	198.42
83.62	54.33	199.28
42.18	54.55	199.61
31.97	54.88	200.76
23.64	---	---
Bulk	53.53	199.48
Experimental	~50	~200

Table S3 Site resolved pair entropy ($S_{(2)}$) contribution in kcal mol^{-1} K^{-1} to the excess entropy ($S_{(ex)}$) of heavy atoms of water and methanol around the distinct structural regions of CT, in various effective dielectric media (ε_{eff})

ε_{eff}	$S_{(2)}$						
	Water			Methanol			
	CT						
	$O_{H_2O} - O_{CX}$	$O_{H_2O} - O_{CX_U}$	$O_{H_2O} - O_{CX_L}$	$O_{MeOH} - O_{CX}$	$O_{MeOH} - O_{CX_U}$	$O_{MeOH} - O_{CX_L}$	$C_{MeOH} - C_{CX_{Aro}}$
95.43	-2.11 (±0.28)	-1.45 (±0.24)	-3.74 (±0.43)	---	---	---	---
86.45	-1.94 (±0.21)	- 1.27 (±0.17)	-3.31 (±0.33)	-0.004 (±0.001)	-0.004 (±0.001)	-0.006 (±0.001)	-0.01 (±0.00)
78.41	-1.38 (±0.13)	-0.94 (±0.09)	-2.21 (±0.21)	-0.008 (±0.002)	-0.008 (±0.003)	-0.02 (±0.00)	-0.03 (±0.00)
40.17	-0.11 (±0.01)	-0.07 (±0.01)	-0.20 (±0.02)	-0.08 (±0.02)	-0.08 (±0.01)	-0.14 (±0.02)	-0.12 (±0.03)
32.45	-0.03 (±0.00)	-0.03 (±0.00)	-0.06 (±0.01)	-0.15 (±0.03)	-0.14 (±0.03)	-0.25 (±0.04)	-0.22 (±0.05)
23.91	---	---	---	-0.51 (±0.08)	-0.54 (±0.09)	-0.81 (±0.11)	-0.73 (±0.14)
	ACT						
95.17	-1.79 (±0.32)	-1.06 (±0.28)	-3.52 (±0.51)	---	---	---	---
87.09	-1.09 (±0.18)	-0.06 (±0.15)	-2.21 (±0.30)	-0.001 (±0.000)	-0.001 (±0.000)	-0.002 (±0.000)	-0.002 (±0.000)
83.62	-0.86 (±0.13)	-0.39 (±0.09)	-2.04 (±0.27)	-0.003 (±0.000)	-0.002 (±0.000)	-0.005 (±0.001)	-0.006 (±0.001)
42.18	-0.09 (±0.01)	-0.05 (±0.01)	-0.21 (±0.03)	-0.06 (±0.02)	-0.04 (±0.01)	-0.13 (±0.02)	-0.082 (±0.026)
31.97	-0.02 (±0.00)	-0.01 (±0.00)	-0.04 (±0.01)	-0.11 (±0.02)	-0.08 (±0.02)	-0.23 (±0.02)	-0.134 (±0.038)

23.64	---	---	---	-0.42 (±0.08)	-0.35 (±0.09)	--0.80 (±0.13)	-0.441 (±0.118)

Table S4 Site resolved diffusion coefficients (in 10^{-5} cm^2/s) of water and methanol from VACF analysis in CT and ACT systems under various ε_{eff}

ε_{eff}	$D^O{}_{H_2O}$			$D^O{}_{MeOH}$		
	Upper	Lower	Aromatic	Upper	Lower	Aromatic
	CT					
95.43	3.89	3.04	4.20	---	---	---
86.45	3.98	4.13	3.62	0.71	---	0.71
78.41	2.24	2.41	3.17	1.89	3.03	2.48
40.17	1.90	2.35	2.48	1.41	1.99	1.81
32.45	1.74	--	2.11	1.48	1.43	1.28
23.91	---	---	---	2.03	1.48	1.73
	ACT					
95.17	4.09	4.06	3.46	---	---	---
87.09	3.61	4.44	3.89	0.66	---	1.49
83.62	2.34	2.72	3.18	2.23	---	1.94
42.18	2.60	3.49	2.18	2.09	2.09	1.87
31.97	1.69	0.32	1.95	1.80	1.54	1.60
23.64	---	---	---	1.59	1.38	1.53

Table S5: Pair entropy ($S_{(2)}$) contribution in kcal mol^{-1} K^{-1} to the excess entropy ($S_{(ex)}$) of oxygen atoms of water and methanol (H_2O(O) and MeOH(O)) and the carbon atom of methanol (MeOH (C)) around calix[4]tyrosol (CT) in various effective dielectric media (ε_{eff}), obtained from the additional independent simulation trajectories.

ε_{eff}	$S_{(2)}$			
	H_2O(O)	MeOH(O)	MeOH(C)	Total
95.43	-3.56 (±0.36)	---	---	-3.56
86.45	-2.59 (±0.21)	-0.01 (±0.00)	-0.01 (±0.00)	-2.61
78.41	-1.79 (±0.13)	-0.01 (±0.00)	-0.02 (±0.00)	-1.82
40.17	-0.14 (±0.01)	-0.13 (±0.01)	-0.12 (±0.02)	-0.39
32.45	-0.04 (±0.00)	-0.22 (±0.02)	-0.21 (±0.03)	-0.47
23.91	---	-0.65 (±0.07)	-0.64 (±0.09)	-1.29

Table S6 Diffusion coefficients (in 10^{-5} cm^2/s) of water and methanol from VACF analysis in CT under various ε_{eff}, obtained from two independent trajectories with standard deviation

ε_{eff}	$D^O{}_{H_2O}$	$D^O{}_{MeOH}$	$D^C{}_{MeOH}$
95.43	4.06 ± 0.005	---	---
86.45	4.02 ± 0.048	0.94 ± 0.014	0.77 ± 0.013
78.41	3.19 ± 0.022	2.11 ± 0.028	2.22 ± 0.003
40.17	2.63 ± 0.035	1.72 ± 0.049	1.74 ± 0.021
32.45	1.68 ± 0.028	1.56 ± 0.042	1.46 ± 0.05
23.91	---	2.04 ± 0.007	2.03 ± 0.091